Stall Spin Flight Path Control Using Parallel Yaw-Periodic Linear Quadratic and Robust H_∞ Controllers

Jeremy W. Hopwood*, James L. Gresham†, and Craig A. Woolsey‡
Virginia Tech, Blacksburg, VA 24060

This paper presents the development and simulation of a robust, periodic linear control law to direct a fixed-wing unmanned aircraft in a stall spin along a desired path. As a flight termination sequence, a spin dissipates energy in a stable, controlled manner. Because control deflections are required to initiate and maintain such a spin, it may be possible, and desirable, to guide the aircraft toward a specific impact location by tilting the, otherwise vertical, axis of the spinning descent. Through augmentation of the dynamics with a measure of velocity vector direction error and the exploitation of a steady spin rate, a yaw-periodic linear quadratic regulator is designed to direct the spin. Then, a robust H_∞ controller is designed for a reduced set of aircraft states and implemented in parallel to robustly maintain the spin in the presence of exogenous disturbances and modeling errors. The combination of the two controllers is shown through simulation of the nonlinear closed-loop system to robustly follow a desired path in the presence of modeling errors and external disturbances.

I. Introduction

It is often required that a fixed-wing unmanned aircraft, such as the RQ-4 Global Hawk, be equipped with an emergency flight termination sequence in the case of a malfunction, such as loss of propulsion or communication [1]. One common flight termination approach is to put the aircraft in a stall spin - a steady descent toward a small and predictable impact location and with a relatively low impact speed as compared to a gliding or spiral descent. Such a termination approach has been used on NASA's Airborne Subscale Transport Aircraft Research (AirSTAR) platform for beyond visual line-of-sight research [2], and is a requirement in the AIAA Student Design, Build, Fly Competition [3]. The main advantage of a spin is that it dissipates energy in a stable, predictable, and controlled manner and thus is an effective failsafe [4].

Still, it is desirable to have the ability to control and direct this spinning descent along a prescribed path to impact in a safe crash zone, as suggested in [5]. This paper presents the development and simulation of a robust, linear control law to direct the spinning descent of an aircraft along a periodic inertial path with a desired average azimuth and inclination angle. The aircraft is controlled by two feedback control laws running in parallel, each with a specialized objective.

First, an infinite-horizon yaw-periodic linear quadratic (LQ) controller computes the optimal input that minimizes a multi-objective cost of cumulative velocity vector error and input/state perturbation from a steady vertical spin. Working in isolation, this controller is effective at controlling the fast yaw dynamics where slowly-parameter-varying assumptions fail. However, this control law tends to command inputs beyond the physical limits of the system when exposed to external disturbances and modeling errors.

Second, a robust H_∞ controller places an upper bound on the worst-case map from exogenous forces, moments, and angular deflections of control surfaces (the LQ controller) to the aircraft's "distance" from the nominal spin (or rather a frequency-dependent weighting of this). The model is assumed to have time-invariant uncertainty in the aerodynamic parameters, representing very real uncertainty and unpredictability of spin aerodynamics [6]. D-K iteration is used to synthesize the robust H_∞ controller, yielding a dynamic output-feedback control law.

The driving factor in this architecture is the need for good tracking while also robustly maintaining a spin. Too much weight on tracking tends to drive the aircraft out of a spin into an unstable dive, while too much weight on perturbation from the vertical spin results in poor tracking of larger desired inclination angles. This paper uses the flight-derived nominal glide model developed in [7] and nominal spin states and control inputs determined from flight data. The developed control law is simulated and shown to have superior performance to a linear quadratic controller alone. Future efforts include flight testing of the control law developed in this paper.

*Graduate Student, Crofton Department of Aerospace and Ocean Engineering, AIAA Student Member, jeremyhopwood@vt.edu
†Graduate Student, Crofton Department of Aerospace and Ocean Engineering, AIAA Senior Member, jamesgresham@vt.edu
‡Professor, Crofton Department of Aerospace and Ocean Engineering, AIAA Associate Fellow, cwoolsey@vt.edu

II. Aircraft Dynamic Model

The aircraft used in the design and simulation of this controller is an E-Flite Carbon-Z Cessna 150 radio-controlled (RC) aircraft, instrumented as described in [7] and [8], as shown in Fig. 1. The aircraft is modeled as a rigid body of mass m with three control surfaces (ailerons, elevators, rudder). It is assumed that the throttle is set to zero during the flight termination maneuver. Let unit vectors $\{\mathbf{i}_1, \mathbf{i}_2, \mathbf{i}_3\}$ define an earth-fixed North-East-Down (NED) orthonormal reference frame, $\mathcal{F}_\mathrm{I}$. Let the unit vectors $\{\mathbf{b}_1, \mathbf{b}_2, \mathbf{b}_3\}$ define the orthonormal body-fixed frame, $\mathcal{F}_\mathrm{B}$, centered at the aircraft center of mass with $\mathbf{b}_1$ pointing along the longitudinal axis out the nose of the aircraft, $\mathbf{b}_2$ out the right wing, and $\mathbf{b}_3$ out the bottom. The position of the body frame with respect to the inertial frame is given by the vector $\mathbf{r} = [x\ y\ z]^\top$. The attitude of the aircraft is given by the rotation matrix, $\mathbf{R}_\mathrm{IB}$, that maps vector components in $\mathcal{F}_\mathrm{B}$ to $\mathcal{F}_\mathrm{I}$. This is described by the 1-2-3 rotation

Fig. 1 E-Flite Carbon-Z Cessna 150.

$$\mathbf{R}_\mathrm{IB} = e^{\hat{\mathbf{e}}_3 \psi} e^{\hat{\mathbf{e}}_2 \theta} e^{\hat{\mathbf{e}}_1 \phi}$$

parameterized by roll (ϕ), pitch (θ), and yaw (ψ) angles, where $\mathbf{e}_1 = [1\ 0\ 0]^\top$, etc., and $\hat{\cdot}$ is the skew-symmetric cross product equivalent matrix satisfying $\hat{\mathbf{a}}\mathbf{b} = \mathbf{a} \times \mathbf{b}$. Let $\mathbf{v} = [u\ v\ w]^\top$ and $\boldsymbol{\omega} = [p\ q\ r]^\top$ be the translational and rotational velocity of the aircraft with respect to $\mathcal{F}_\mathrm{I}$ expressed in $\mathcal{F}_\mathrm{B}$, respectively. With this choice of Euler angles, we have the kinematic equations of motion

$$\dot{\mathbf{r}} = \mathbf{R}_\mathrm{IB}\mathbf{v} \tag{1a}$$

$$\dot{\mathbf{R}}_\mathrm{IB} = \mathbf{R}_\mathrm{IB}\hat{\boldsymbol{\omega}} \tag{1b}$$

With $\boldsymbol{\Theta} := [\phi\ \theta\ \psi]^\top$, Eq. (1b) becomes

$$\dot{\boldsymbol{\Theta}} = \mathbf{L}_\mathrm{IB}\boldsymbol{\omega} = \begin{bmatrix} 1 & \sin\phi\tan\theta & \cos\phi\tan\theta \\ 0 & \cos\phi & -\sin\phi \\ 0 & \sin\phi\sec\theta & \cos\phi\sec\theta \end{bmatrix} \begin{bmatrix} p \\ q \\ r \end{bmatrix} \tag{2}$$

Let us represent the aerodynamic forces and moments on the aircraft expressed in $\mathcal{F}_\mathrm{B}$ as $\mathbf{F}_\mathrm{aero} = [X\ Y\ Z]^\top$ and $\mathbf{M}_\mathrm{aero} = [\mathscr{L}\ \mathscr{M}\ \mathscr{N}]^\top$. Define $\mathbf{p} = m\mathbf{v}$ to be the linear momentum of the aircraft and $\mathbf{h} = \mathbf{I}\boldsymbol{\omega}$ to be the angular momentum vector about the center of mass, both expressed in $\mathcal{F}_\mathrm{B}$. Here, $\mathbf{I}$ is the moment of inertia matrix about the center of mass in $\mathcal{F}_\mathrm{B}$. Thus, we have the dynamic equations of motion

$$\begin{aligned} \dot{\mathbf{p}} &= \mathbf{p} \times \boldsymbol{\omega} + mg\mathbf{R}_\mathrm{BI}\mathbf{e}_3 + \mathbf{F}_\mathrm{aero} \\ \dot{\mathbf{h}} &= \mathbf{h} \times \boldsymbol{\omega} + \mathbf{M}_\mathrm{aero} \end{aligned} \tag{3}$$

Requiring a high-fidelity spin aerodynamic model in order to design the proposed model-based flight termination strategy would be unrealistic for most aircraft. For this reason, a nonlinear aerodynamic model is used which was validated for perturbations from nominal, wings-level, gliding flight. The details of which are found in [7]. The body-frame forces and moments are functions of airspeed, $V = \|\mathbf{v}\|$, angle-of-attack, α, angle-of-sideslip, β, and body angular velocity, $\boldsymbol{\omega}$. Here, α and β are defined by the transformation from the wind frame, $\mathcal{F}_\mathrm{W}$, to the body frame, given by

$$\mathbf{R}_\mathrm{BW} = e^{-\hat{\mathbf{e}}_2 \alpha} e^{\hat{\mathbf{e}}_3 \beta}$$

For control surface deflections $\boldsymbol{\delta} = [\delta_a\ \delta_e\ \delta_r]^\top$, the nonlinear aerodynamic model is a function of the aircraft states and inputs in the form

$$\begin{aligned} \mathbf{F}_\mathrm{aero} &= \mathbf{F}_\mathrm{aero}\,(V, \alpha, \beta, \boldsymbol{\omega}, \boldsymbol{\delta}) \\ \mathbf{M}_\mathrm{aero} &= \mathbf{M}_\mathrm{aero}\,(V, \alpha, \beta, \boldsymbol{\omega}, \boldsymbol{\delta}) \end{aligned}$$

A nominal stall spin is steady in yaw angle (ignoring position), so we define the *reduced state* vector, $\mathbf{x}_r$, to be the states that are constant in a spin, i.e. roll and pitch angle, body velocity (or wind-frame), and body angular velocity. We desire the nominal spin to be a steep stall spin with aileron, elevator, and rudder at about 75% maximum deflection. These two requirements correspond to control surface deflections that are not too close to the saturation limits, but also result in a relatively low angle-of-attack to maintain aerodynamic control authority. With an aerodynamic model, the nominal spin can readily be found using the model-based methods detailed in [9] and [10].

However, for the aircraft presented here, nominal spin flight data were collected in conjunction with the aerodynamic system identification flight tests discussed in [7]. Steady nominal spin state and control input values determined from flight data are

$$\begin{array}{llll} \tilde{\phi} = -24.01 \text{ deg} & \tilde{V} = 20.40 \text{ m/s} & \tilde{p} = -384.5 \text{ deg/s} & \tilde{\delta}_a = 15.5 \text{ deg} \\ \tilde{\theta} = -73.96 \text{ deg} & \tilde{\alpha} = 12.38 \text{ deg} & \tilde{q} = 36.23 \text{ deg/s} & \tilde{\delta}_e = -18.5 \text{ deg} \\ & \tilde{\beta} = 5.74 \text{ deg} & \tilde{r} = -97.17 \text{ deg/s} & \tilde{\delta}_r = 24.6 \text{ deg} \end{array} \tag{4}$$

where $\tilde{\cdot}$ denotes the nominal quantity. Note that the nominal values given in Eq. (4) do not correspond precisely to an equilibrium of the reduced system, but will be very close. The consequences of this observation are further discussed at the end of Section III.C.

For the nominal spin chosen, yaw angle takes the form

$$\tilde{\psi}(t) = \psi_0 + \tilde{\Omega} t \tag{5}$$

where from Eq. (2), we have the nominal spin rate

$$\tilde{\Omega} := \dot{\tilde{\psi}} = \tilde{q} \sin\tilde{\phi} \sec\tilde{\theta} + \tilde{r} \cos\tilde{\phi} \sec\tilde{\theta} \approx -399 \, \frac{\text{deg}}{\text{s}}$$

The vertical descent rate is steady with

$$\dot{\tilde{z}} = -\tilde{u} \sin\tilde{\theta} + \tilde{v} \sin\tilde{\phi} \cos\tilde{\theta} + \tilde{w} \cos\tilde{\phi} \cos\tilde{\theta} \approx 19.6 \, \frac{\text{m}}{\text{s}}$$

The lateral displacement is obtained from

$$\begin{aligned} \dot{x} &= -C_1 \sin\psi + C_2 \cos\psi \\ \dot{y} &= C_2 \sin\psi + C_1 \cos\psi \end{aligned}$$

where C_1 and C_2 are constant for the nominal spin, taken from Eq. (1a). Thus for the nominal motion, we have

$$\begin{aligned} \tilde{x}(t) &= x_0 + \frac{1}{\tilde{\Omega}} \left(C_1(\cos\psi - \cos\psi_0) + C_2(\sin\psi - \sin\psi_0) \right) \\ \tilde{y}(t) &= y_0 + \frac{1}{\tilde{\Omega}} \left(-C_2(\cos\psi - \cos\psi_0) + C_1(\sin\psi - \sin\psi_0) \right) \end{aligned} \tag{6}$$

where x_0, y_0, and ψ_0 are the initial conditions of x, y, and ψ, respectively.

III. Controller Design

A. Approach

We choose to define the desired path to be a constant unit vector, defined from the initiation of the spin, pointing in some desired direction. The aim is to slant the centerline of this helical descent to converge on the specified line. This desired path is minimally represented by an azimuth angle, φ_d, and inclination angle, ϑ_d. As a vector in the inertial frame, $\mathcal{F}_\text{I}$, this direction is denoted $\boldsymbol{\sigma}_d$. The goal of the controller is to make the the perpendicular distance between the aircraft center of mass and the desired path small, while ensuring the aircraft state variable values remain sufficiently close to values that correspond to the the nominal spin.

Remark 1 Some major challenges are

(i) *An accurate aerodynamic model for a spin is generally not readily known.*

(ii) *Control surface deflections are easily saturated in a spin.*

(iii) *For a skewed helical spin about the desired path, the cross-track error is not identically zero.*

(iv) *Yaw angle has fast dynamics that are non-trivial to control with a linear approach. For a control law designed based on a time-varying linearization, yaw angle will drift during perturbations from the nominal state so that the small perturbation model becomes inaccurate over time.*

The dynamics are augmented with the integral of the error between the desired and actual velocity vector directions to address (iii). Through an independent variable change, a yaw-periodic linear quadratic (LQ) regulator is designed to address (iv). Then, a stationary H_∞ controller is designed for the reduced dynamics to address (i) and (ii). For these reasons, we choose the control architecture shown in Figure 2, where Δ is an operator that belongs to a chosen uncertainty set $\mathbf{\Delta}$, G is the performance-based system, $\mathbf{K}_\infty$ is the dynamic H_∞ controller, $\mathbf{K}(\psi)$ is the yaw-periodic LQ state feedback gain, $\mathbf{y}$ are the measurements, $\mathbf{z}$ are the performance outputs which we want to make small, and $\mathbf{d}$ are the exogenous force and moment disturbances to the system. Note we now denote $\delta(\cdot)$ to be the perturbation from $\tilde{\cdot}$ for the linearization about the nominal spin.

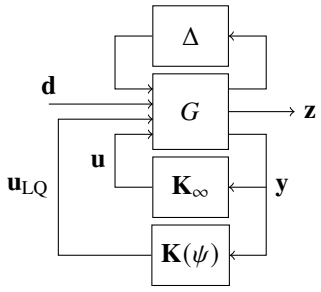

Fig. 2 Parallel control architecture.

B. Yaw-Periodic Linear Quadratic Regulator

To address the periodic nature of the cross-track error dynamics, we choose to augment the system with a state that represents the integral error between the desired and actual velocity vector directions. The velocity vector direction expressed in $\mathcal{F}_\mathrm{I}$ is

$$\boldsymbol{\sigma}_i = \mathbf{R}_\mathrm{IW}\mathbf{e}_1$$

where $\mathbf{R}_\mathrm{IW} = \mathbf{R}_\mathrm{IB}\mathbf{R}_\mathrm{BW}$. Because the desired path is a line, the perpendicular cross-track error can be defined by the projection of the position vector onto $\boldsymbol{\sigma}_d$ by

$$\mathbf{e}_\perp = \left(\mathbf{r}^\top\boldsymbol{\sigma}_d\right)\boldsymbol{\sigma}_d - \mathbf{r}$$

as shown in Figure 3. We then define the corrected velocity vector direction, $\boldsymbol{\sigma}_c$, to be the unit vector that points from the aircraft to a point on the desired path some look-ahead distance, k, ahead of perpendicular. This is illustrated in Figure 3 and expressed as

$$\boldsymbol{\sigma}_c = \frac{\mathbf{e}_\perp + k\boldsymbol{\sigma}_d}{\|\mathbf{e}_\perp + k\boldsymbol{\sigma}_d\|}$$

The correction of the velocity vector direction is introduced to ensure the spin axis of the convergent trajectory is on the path as opposed to parallel to it. Then, defining $\mathbf{e}_v$ to be the integral error between the desired and actual velocity vector directions, we have

$$\dot{\mathbf{e}}_v = \boldsymbol{\sigma}_i - \boldsymbol{\sigma}_c \tag{7}$$

We now write the augmented equations of motion from Eqs. (2), (3), and (7) as

$$\dot{\mathbf{\Theta}} = \mathbf{L}_\mathrm{IB}\boldsymbol{\omega} \tag{8a}$$

$$\dot{\mathbf{v}} = \mathbf{v}\times\boldsymbol{\omega} + g\mathbf{R}_\mathrm{BI}\mathbf{e}_3 + \frac{1}{m}\mathbf{F}_\mathrm{aero} \tag{8b}$$

$$\dot{\boldsymbol{\omega}} = \mathbf{I}^{-1}\left(\mathbf{I}\boldsymbol{\omega}\times\boldsymbol{\omega} + \mathbf{M}_\mathrm{aero}\right) \tag{8c}$$

$$\dot{\mathbf{e}}_v = \boldsymbol{\sigma}_i - \boldsymbol{\sigma}_c \tag{8d}$$

Linearizing these dynamics about the nominal spinning motion gives a T-periodic linear state equation, where $T = |360/\tilde{\Omega}| \approx 0.9$ s. Since ψ is the "fast" variable in this motion, the true yaw angle can quickly become out of phase with the nominal yaw angle for perturbations from $\tilde{\psi}(t)$. This results in poor azimuth tracking by a T-periodic controller. We consider the dynamics in Eq. (8) where the position $\mathbf{r}$, appearing only in $\boldsymbol{\sigma}_c$, is assumed nominal as a function

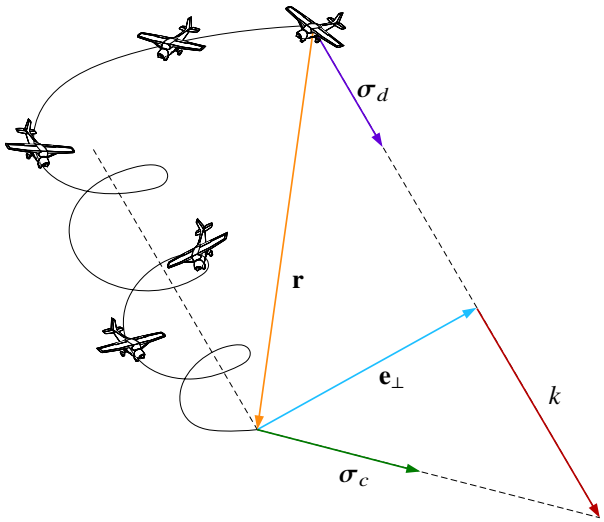

Fig. 3 Cross-track error, $\mathbf{e}_\perp$, and corrected desired velocity vector direction, σ_c.

of yaw angle, $\tilde{\mathbf{r}}(\psi)$. Note that Eqs. (8a), (8b), and (8c) are time-invariant and $\tilde{\psi}(t)$ is the only time-varying nominal state variable that explicitly appears in the dynamics. Because $\psi(t)$ increases monotonically in time during a spinning descent, we may consider ψ to be the independent variable for the system

$$\mathbf{x}'(\psi) = \frac{1}{\tilde{\Omega}} \begin{bmatrix} \mathbf{f}_{x,r}(\mathbf{x}_r, \mathbf{u}_{\mathrm{LQ}}) \\ \mathbf{f}_{e,v}(\tilde{\mathbf{r}}(\psi), \mathbf{x}_r, \psi) \end{bmatrix} \tag{9}$$

where $\mathbf{x} := [\mathbf{x}_r^\top \ \mathbf{e}_v^\top]^\top$ and $(\cdot)' = \frac{\mathrm{d}(\cdot)}{\mathrm{d}\psi}$. When $\psi = \tilde{\psi}(t) = \tilde{\Omega}t$, this system produces trajectories in ψ that are a linear transformation away (Eq. (5)) from those of the original system in time. From Eq. (9), we have the 2π-periodic linearization in ψ,

$$\delta\mathbf{x}'(\psi) = \mathbf{A}_a(\psi)\delta\mathbf{x}(\psi) + \mathbf{B}_a\delta\mathbf{u}_{\mathrm{LQ}}(\psi) \tag{10}$$

where δ denotes a perturbation from the nominal value. Eq. 10 is the linear state equation for which the yaw-varying LQ controller is designed. The linear-quadratic regulator problem is to determine the control, $\mathbf{u}_{\mathrm{LQ}}$, that minimizes

$$J = \lim_{\psi_f \to \infty} \int_0^{\psi_f} \left(\delta\mathbf{u}_{\mathrm{LQ}}^\top(\psi)\mathbf{R}\delta\mathbf{u}_{\mathrm{LQ}}(\psi) + \delta\mathbf{x}^\top(\psi)\mathbf{Q}\delta\mathbf{x}(\psi) \right) \mathrm{d}\psi$$

subject to Eq. (10) and initial condition $\delta\mathbf{x}(0) = \delta\mathbf{x}_0$ where we choose

$$\mathbf{Q} = \begin{bmatrix} \mathrm{diag}(\delta\mathbf{x}_{r,\max})^{-1} & \mathbf{0} \\ \mathbf{0} & \nu\,\mathbb{I}_3 \end{bmatrix} \qquad \mathbf{R} = \rho\,\mathrm{diag}(\delta\mathbf{u}_{\max})^{-1}$$

with $\mathbb{I}_n$ representing the $n \times n$ identity matrix. Here $\delta(\cdot)_{\max}$ represents soft perturbation limits by which $\mathbf{Q}$ and $\mathbf{R}$ are normalized. Here ν and ρ are positive weightings that determine the balance of the 3 objectives: reduced state perturbation, input perturbation, and cross-track error. Let $\mathbf{P}(\psi, \psi_f)$ be the solution of the differential Riccati equation, $-\dot{\mathbf{P}} = \mathbf{A}_a^\top\mathbf{P} + \mathbf{P}\mathbf{A}_a - \mathbf{P}\mathbf{B}_a\mathbf{R}^{-1}\mathbf{B}_a^\top\mathbf{P} + \mathbf{Q}$, with $\mathbf{P}(\psi_f) = \mathbf{0}$. Since $\mathbf{A}_a(\psi)$ is bounded and continuous and the pair $(\mathbf{A}_a, \mathbf{B}_a)$ is controllable, $\mathbf{P}(\psi, \psi_f)$ converges to some bounded, positive semi-definite $\overline{\mathbf{P}}(\psi)$ as $\psi_f \to \infty$ [11]. Then the solution to the LQ control design problem is

$$\delta\mathbf{u}_{\mathrm{LQ}}(\psi) = -\mathbf{R}^{-1}\mathbf{B}_a^\top\bar{\mathbf{P}}(\psi)\delta\mathbf{x}(\psi) = -\mathbf{K}(\psi)\delta\mathbf{x}(\psi) \tag{11}$$

Values for the three control parameters, ν, ρ, and k, are chosen through simulation of the LQ controller alone (without disturbances and model perturbations) such that inputs are not saturated and there is a good balance between

reduced state perturbation from the nominal spin and cross-track error. This controller tuning is done iteratively while increasing the desired inclination angle until the LQ controller is no longer capable of achieving the desired motion. From these results, we choose $\nu = 1$, $\rho = 1$, and $k = 150$ m and find the maximum inclination angle is approximately $\vartheta_{\max} = 25°$. The numerically approximated steady-state solution of the Riccati equation yields a feedback gain, $\mathbf{K}(\psi)$, where each term is either constant or sinusoidal in ψ with a period of 2π.

C. Robust H_∞ Controller

An H_∞ controller is now designed for the reduced state dynamics. Since the aerodynamics are uncertain, the control law is designed to be robust to the uncertainty of aerodynamic model parameters. We assume the uncertainty acts on the plant, G, as a linear bounded operator, Δ, in a way that represents time-invariant uncertainty in the 37 aerodynamic parameters found in the nominal glide model in [7]. We assume three inputs affect the system: inputs commanded by the LQ controller, $\mathbf{u}_{\text{LQ}}$, force and moment disturbances, $\mathbf{d}$, and the remaining control inputs to be assigned according to the H_∞ control law, $\mathbf{u}$. The force and moment disturbances are assumed to be finite-time square-integrable ($\mathbf{d} \in L_{2,e}$) and the commanded inputs from the LQ controller, $\mathbf{u}_{\text{LQ}}$, is an exogenous, measurable signal. This gives the linear state equation

$$P: \quad \delta\dot{\mathbf{x}}_r = \mathbf{A}_r\delta\mathbf{x}_r + \mathbf{B}_r(\delta\mathbf{u}_{\text{LQ}} + \delta\mathbf{u}) + \mathbf{B}_d\mathbf{d}$$

with measurements $\mathbf{y} = \begin{bmatrix}\delta\mathbf{x}_r^\top & \delta\mathbf{u}_{\text{LQ}}^\top\end{bmatrix}^\top$. For now, consider the nominal system, where the uncertainty operator, Δ, is ignored. We define the scaled exogenous disturbances, $\mathbf{w}$, and performance outputs, $\mathbf{z}$, respectively, in the frequency domain as

$$\mathbf{w}(s) = \begin{bmatrix}\mathbf{W}_d(s) & \mathbf{0}\\ \mathbf{0} & \mathbf{W}_{\text{LQ}}(s)\end{bmatrix}\begin{bmatrix}\mathbf{d}(s)\\ \delta\mathbf{u}_{\text{LQ}}(s)\end{bmatrix} \qquad \mathbf{z}(s) = \begin{bmatrix}\mathbf{W}_x(s) & \mathbf{0}\\ \mathbf{0} & \mathbf{W}_u(s)\end{bmatrix}\begin{bmatrix}\delta\mathbf{x}_r(s)\\ \delta\mathbf{u}(s)\end{bmatrix}$$

where $\mathbf{W}_d$, $\mathbf{W}_{\text{LQ}}$, $\mathbf{W}_x$, and $\mathbf{W}_u$ are frequency-dependent scalings based on maximum allowable/expected values of the corresponding variables. Adopting standard notation, this system is now expressed as

$$G(s) = \left[\begin{array}{c|c} G_{11} & G_{12}\\ \hline G_{21} & G_{22}\end{array}\right] := \left[\begin{array}{c|cc} \mathbf{A}_r & [\mathbf{B}_d\ \ \mathbf{B}_r] & \mathbf{B}_r\\ \hline \mathbf{C}_z & \mathbf{0} & \mathbf{D}_{zu}\\ \mathbf{C}_y & \mathbf{D}_{yw} & \mathbf{0}\end{array}\right] := \begin{bmatrix}\mathbf{C}_z\\ \mathbf{C}_y\end{bmatrix}(s\mathbb{I} - \mathbf{A}_r)^{-1}\begin{bmatrix}\mathbf{B}_w & \mathbf{B}_r\end{bmatrix} + \begin{bmatrix}\mathbf{0} & \mathbf{D}_{zu}\\ \mathbf{D}_{yw} & \mathbf{0}\end{bmatrix}$$

For the control law synthesis and simulation results in this paper, the maximum allowable reduced state perturbation and maximum expected forces and moments are taken from spin system identification maneuvers. Flight data collection in [7] includes maneuvers during which the nominal spin is intentionally perturbed by additional inputs, with the aim of identifying aerodynamic model parameters in the spin regime, but without causing the aircraft to recover from the spin.

Let $\mathbf{W}_d$, $\mathbf{W}_u$, and $\mathbf{W}_{\text{LQ}}$ be constant scalings, where $\mathbf{W}_{\text{LQ}} = \mathbf{W}_u^{-1}$, and $\mathbf{W}_x$ is a weighted 10 Hz first-order low-pass filter. The disturbance weightings, $\mathbf{W}_d$ and $\mathbf{W}_{\text{LQ}}$, and the maximum reduced state perturbation, $\delta\mathbf{x}_{r,\max}$, are all determined independently from the same trajectory with control surface deflections which we denote $\boldsymbol{\delta}_{\text{excite}}$. As a consequence, trajectories under maximum expected force and moment disturbances in addition to control inputs $\boldsymbol{\delta}_{\text{excite}}$ result in reduced state perturbations, $\delta\mathbf{x}_r$, nearly double the designed maximum, $\delta\mathbf{x}_{r,\max}$. Therefore, $\mathbf{W}_d$ and $\mathbf{W}_{\text{LQ}}$ are scaled by a weighting factor, $\lambda \in (0, 1)$, which represents the weighting of force/moment disturbance rejection relative to the LQ controller attenuation. This weighting, as shown in Figure 4, gives a realistic performance criterion which we want robustly satisfied. As λ approaches 0, the H_∞ controller only minimizes the effect LQ inputs have on $\mathbf{z}$. Conversely, as λ approaches 1, the H_∞ controller minimizes only the effect of disturbances on $\mathbf{z}$. For simulation, we choose a disturbance weighting of $\lambda = 0.5$ to equally weight force/moment rejection and LQ controller attenuation.

Let $M = \underline{S}(G, K)$ be the closed-loop, transfer function from $\mathbf{w}$ to $\mathbf{z}$, including the effects of the uncertainty operator, Δ. This is described by the lower linear fractional transformation $\underline{S}(G, K) = G_{11} + G_{12}K\left(I - G_{22}K\right)^{-1}G_{21}$. Assuming M has the structure

$$M = \left[\begin{array}{c|c} M_{11} & M_{12}\\ \hline M_{21} & M_{22}\end{array}\right]$$

with inputs/outputs of M being the outputs/inputs of Δ, the inclusion of the uncertainty operator is described by the upper linear fractional transformation $\overline{S}(M, \Delta) = M_{22} + M_{21}\Delta\left(I - M_{11}\Delta\right)^{-1}M_{12}$, where M_{22} is the nominal closed-loop

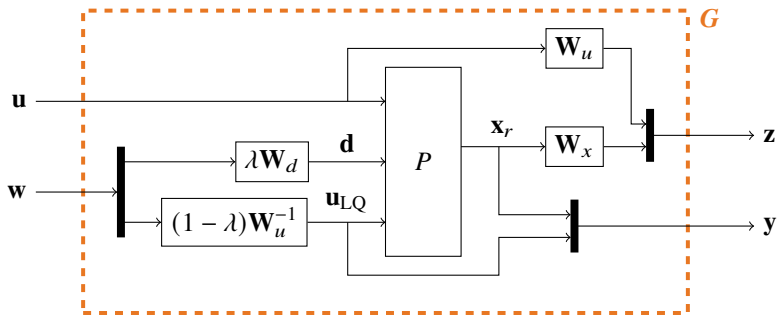

Fig. 4 H_∞ weighted block diagram.

system from $\mathbf{w} \mapsto \mathbf{z}$. For internally stable $\delta\dot{\mathbf{x}}_{r,\text{cl}} = M_{22}\delta\mathbf{x}_{r,\text{cl}}$, where $\delta\mathbf{x}_{r,\text{cl}}$ is the closed-loop reduced state perturbation, the uncertain system M is *robustly stable* when $(I - M_{11}\Delta)^{-1}$ exists for all $\Delta \in \mathbf{\Delta}$ [12].

When there is no uncertainty, the H_∞ problem is to find a controller, K, that minimizes the upper bound on the worst-case map from $\mathbf{w}$ to $\mathbf{z}$. Specifically, we want the induced L_2 norm of the closed loop system to satisfy

$$\|G_{\text{cl}}\|_\infty = \|G_{\text{cl}}\|_{L_2 \to L_2} = \operatorname*{ess\,sup}_{\omega \in \mathbb{R}} \overline{\sigma}(\hat{G}_{\text{cl}}(j\omega)) < \gamma \leq 1 \tag{12}$$

where $\hat{G}_{\text{cl}}(j\omega)$ is the frequency domain description of G_{cl} and $\overline{\sigma}(\cdot)$ is the largest singular value. Let $\mathcal{K}$ be the set of stabilizing controllers. The problem is to find

$$\arg\inf_{K \in \mathcal{K}} \|\underline{S}(G, K)\|_\infty < \gamma \tag{13}$$

where γ is the H_∞ performance measure. A value of γ less than 1 indicates the closed-loop performance is contractive and our desired criterion is met.

Regarding model uncertainty, we assume the aerodynamic parameters take on values within the 95% confidence intervals, determined from the model identification process in [7]. We choose the time-invariant uncertainty set

$$\mathbf{\Delta} := \left\{\text{diag}(\Delta_1, \cdots, \Delta_p) \mid \Delta_i \in \mathcal{L}^c_{\text{TI}}(L_2),\ \|\Delta_i\|_\infty < 1\right\}$$

where $\mathcal{L}^c_{\text{TI}}(L_2)$ is the set of causal, time-invariant, linear bounded operators on the space of square-integrable functions, L_2. Let $\mathcal{D}$ be the set of time-invariant non-zero scalings that commute with the uncertainty set, $\mathbf{\Delta}$, as shown in [12] to be

$$\mathcal{D} = \left\{D \in \mathcal{L}^c_{\text{TI}}(L_2) \mid D \text{ non-singular},\ \hat{D}(s) = \text{diag}(\hat{D}_1(s)\mathbb{I}, \cdots, \hat{D}_d(s)\mathbb{I})\right\}$$

where each $\hat{D}_i(s) \in \text{RH}_\infty$ (the space of proper transfer functions with no poles in the closed right-half of the complex plane). With the chosen structured uncertainty, analysis and synthesis of the controller is readily conducted using the structured singular value, μ. For the uncertain system, M, and the given uncertainty set, $\mathbf{\Delta}$, the structured singular value, μ, satisfies

$$\mu(M_{11}, \mathbf{\Delta}) = \frac{1}{\inf\{\|\Delta\|_\infty \mid \Delta \in \mathbf{\Delta},\ (I - M_{11}\Delta) \text{ singular}\}} \leq \inf_{D \in \mathcal{D}} \|\hat{D}\hat{M}_{11}\hat{D}^{-1}\|_\infty$$

as shown in [13]. The robustly stable system has *robust performance* if $\mu(M_{11}, \mathbf{\Delta}) < 1$, meaning the performance measure remains contractive for all structured uncertainty within the bounds determined in the modeling process. Thus, the problem is to find

$$\arg\inf_{K \in \mathcal{K},\, D \in \mathcal{D}} \|\hat{D}\hat{M}_{11}\hat{D}^{-1}\|_\infty \leq \mu \tag{14}$$

This is in general a non-convex problem, so we use D-K iteration to find a local minimum using the MATLAB® Robust Control Toolbox [14] [15]. This computation yields an upper bound on the structured singular value of $\mu = 0.9066$. Thus, the H_∞ norm of the closed-loop linear system remains below μ for all normalized structured uncertainty of $1/\mu$. The uncontrolled and closed loop singular value plots for a variety of uncertain parameter values are shown in Figures 5a and 5b.

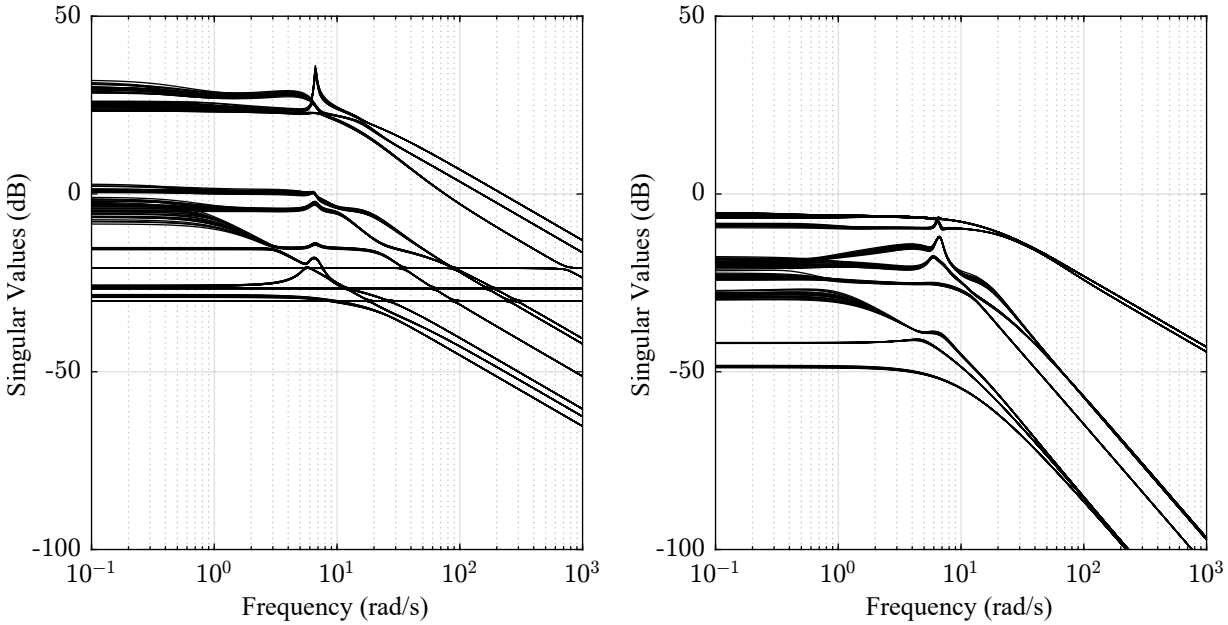

(a) Uncontrolled singular values **(b) Closed-loop singular values**

Fig. 5 Singular value comparison.

Proposition 1 *The closed-loop, reduced linear system, given by the control formulations in Eqs.* (11) *and* (14) *and the connection in Figure 2, is robustly stable.*

Proof. By the μ-synthesis result of $\mu < 1$, the closed loop reduced system is robustly stable. This holds true for exogenous signals $\mathbf{w}$ in extended L_2 space, $L_{2,e}[0, t_1]$, which satisfy

$$\int_0^{t_1} \|\mathbf{w}(t)\|_2^2 \, \mathrm{d}t < \infty$$

for all finite $t_1 \geq 0$. The disturbance $\mathbf{d}$ is assumed in $L_{2,e}$, and signal $\mathbf{u}_{\mathrm{LQ}}$ is generated by the linear, bounded state feedback gain, $\mathbf{K}(\psi)$, and thus, is also in $L_{2,e}$. Therefore, the closed loop linear system is robustly stable. □

As for the closed-loop model of the nonlinear system, the point about which the reduced system is linearized is not an equilibrium. Therefore, an internally stabilizing linear controller results in closed loop trajectories for which the time-derivative of the states is non-zero. For the nominal spinning motion (which corresponds to the origin of the linear system), this is effectively equivalent to a bounded exogenous disturbance, which is robustly rejected by the H_∞ controller. While the region of attraction for the nonlinear closed-loop system is unknown, the robustness and performance is evaluated through simulation.

IV. Simulation and Results

The nonlinear closed loop dynamics are simulated, incorporating control deflection bounds, wind disturbances, and perturbations from the nominal glide aerodynamic model in [7]. We illustrate the performance of this control law through the following scenario. Suppose the Carbon-Z Cessna 150 initiates a spinning flight termination sequence with the spin fully developed at 1000 ft above ground level. There is constant 15 knot wind from the West. Through some algorithm, it is determined the best safe crash zone is 350 ft due Northeast, corresponding to approximately a 20.5° desired inclination angle. To demonstrate robustness, the aerodynamic parameters are arbitrarily taken as the value halfway between their estimate and upper 95% confidence interval. These parameter values are used in simulation, while the control law is synthesized using the modeled parameter estimates.

Consider the closed-loop response under the yaw-periodic LQ controller, as shown in Figure 6a, where the desired path is shown as the solid black line. The aircraft begins to track the desired path, but then exits the spin. The LQ controller cannot reject the wind disturbance and model perturbations, failing to keep the aircraft in the spin. To combat

the lack of robustness and tendency to exit the spin, we now add the H_∞ controller in parallel. The closed-loop parallel response is shown in Figure 6b, displaying good tracking of the desired path while maintaining a spin. This scenario demonstrates the benefit of the parallel control architecture. The norm of the reduced state perturbation for each case, as well as constant spin inputs, is shown in Figure 7. Both the LQ and H_∞ controllers penalize perturbations from the nominal spin, but the addition of the H_∞ control law adds robustness and a performance-based result to satisfy this requirement.

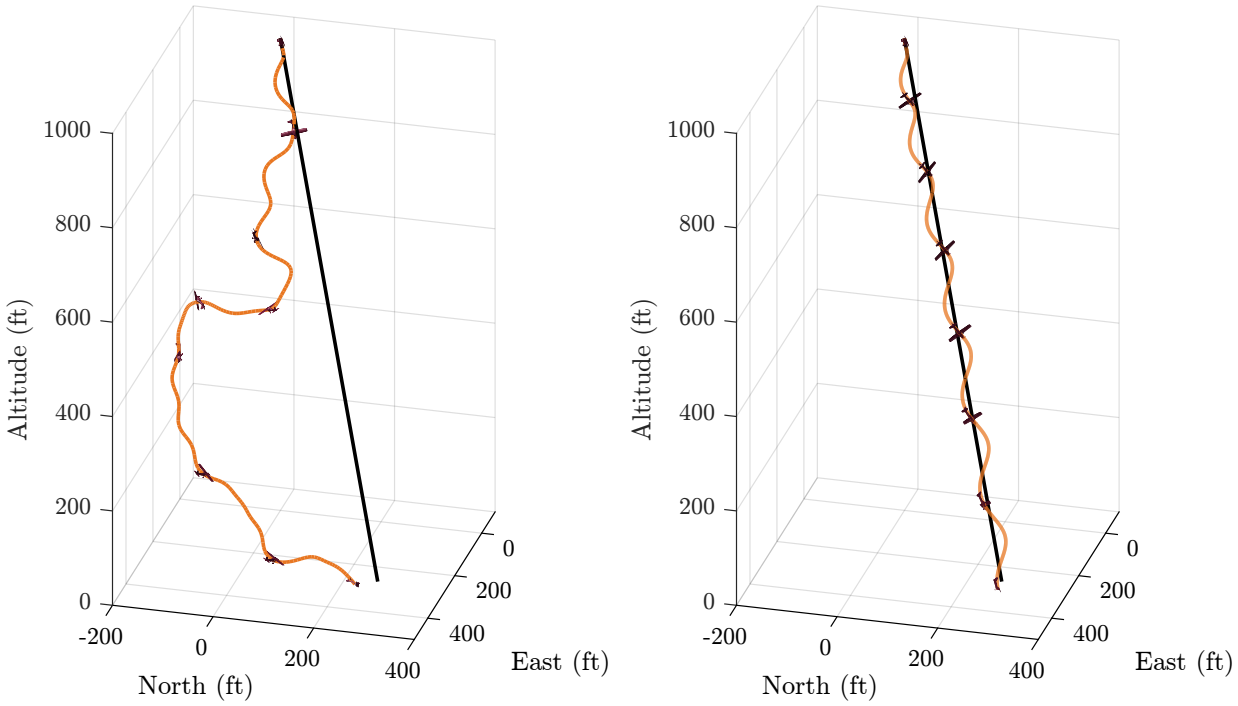

(a) LQ controller response **(b) Parallel (LQ + H_∞) controller response**

Fig. 6 LQ vs. parallel controller simulated with wind and model perturbations.

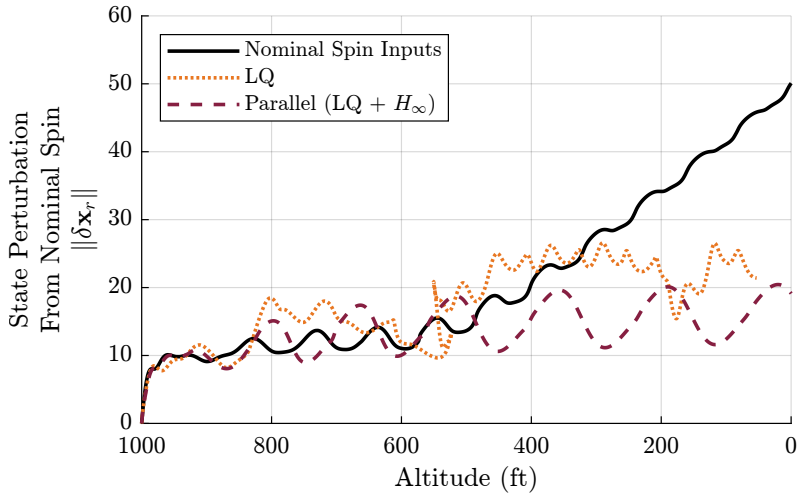

Fig. 7 Reduced state perturbation.

V. Conclusions and Future Work

The development and simulation of a robust, linear control law to direct the spinning descent of an aircraft along a desired azimuth and inclination angle is presented. This control law, implemented as a fixed-wing UAS flight termination sequence, can direct the aircraft towards a safe crash zone in a controlled manner with a small crash radius, thereby reducing the likelihood and severity of a collision with persons or property on the ground.

The proposed linear control law combines the advantages of a state-varying linear quadratic regulator and a time-invariant robust H_∞ controller in a parallel implementation. The result is a control law that robustly maintains a spinning descent, while also directing the aircraft's path along a desired direction. In simulations of the nonlinear dynamics, the control law shows good disturbance rejection as well as robustness to changes in the aerodynamic model. This is especially important as the aerodynamics in a spin are not captured well by a nominal glide flight model [7].

One drawback of the presented control law is the inclusion of only soft constraints on input saturation. Similarly, dynamic constraints on the aircraft states that would precisely keep the aircraft in a spin are not identified - only weightings taken from flight data. Ongoing efforts include the validation of the nominal glide derived controller with an accurate nonlinear spin model, as well as a flight test program using both nominal glide and spin aerodynamic models.

Acknowledgments

The authors gratefully acknowledge the support of NASA under Grant No. 80NSSC20M0162 and the Center for Unmanned Aircraft Systems, an NSF Industry/University Cooperative Research Center under NSF Grant No. CNS-1650465.

References

[1] Kinzig, B., "Global Hawk systems engineering case study," Tech. rep., Air Force Center for Systems Engineering, AFIT, 2009.

[2] Cunningham, K., Cox, D. E., Foster, J. V., Riddick, S. E., and Laughter, S. A., "AirSTAR beyond visual range UAS description and preliminary test results," *AIAA Guidance, Navigation, and Control Conference*, 2016, pp. 1–14. https://doi.org/10.2514/6.2016-0882.

[3] American Institute of Aeronautics and Astronautics, "2020-21 Design, Build, Fly Rules," Tech. rep., AIAA, 2020. URL https://www.aiaa.org/dbf/competition-information/rules-resources.

[4] Stansbury, R. S., Tanis, W., and Wilson, T. A., "A technology survey of emergency recovery and flight termination systems for UAS," *AIAA Infotech*, 2009, pp. 1–8. https://doi.org/10.2514/6.2009-2038.

[5] Carney, E., Castano, L., and Xu, H., "Determination of safe landing zones for an autonomous UAS using elevation and population density data," *AIAA SciTech Forum*, 2019, pp. 1–16. https://doi.org/10.2514/6.2019-1060.

[6] Murch, A. M., "Aerodynamic Modeling of Post-Stall and Spin Dynamics of Large Transport Airplanes," *Master's Thesis, Aerospace Engineering, Georgia Institute of Technology*, 2007.

[7] Gresham, J. L., Simmons, B. M., Hopwood, J. W., and Woolsey, C. A., "Spin aerodynamic modeling for a fixed-wing aircraft using flight data," *AIAA SciTech Forum*, 2022, To appear, pp. 1–16.

[8] Gresham, J. L., Fahmi, J.-M., Simmons, B. M., Hopwood, J. W., Foster, J. W., and Woolsey, C. A., "Flight test approach for modeling and control law validation for unmanned aircraft," *AIAA SciTech Forum*, 2022, To appear, pp. 1–23.

[9] Shukla, P. J., "Active Flight Path Control for an Induced Spin Flight Termination System," *Master's Thesis, Virginia Polytechnic Institute and State University, Engineering Science and Mechanics*, 2017.

[10] Shukla, P., and Woolsey, C. A., "Active flight path control in a stall-spin flight termination system," *AIAA SciTech Forum*, 2018, pp. 1–18. https://doi.org/10.2514/6.2018-0528.

[11] Kalman, R. E., "When is a linear control system optimal?" *Journal of Fluids Engineering, Transactions of the ASME*, Vol. 86, No. 1, 1964, pp. 51–60. https://doi.org/10.1115/1.3653115.

[12] Dullerud, G. E., and Paganini, F., *A Course in Robust Control Theory: A Convex Approach*, Springer, 2000. https://doi.org/10.1007/978-1-4757-3290-0.

[13] Packard, A., Doyle, J., and Balas, G., "Linear, multivariable robust control with a μ perspective," *Journal of Dynamic Systems, Measurement and Control, Transactions of the ASME*, Vol. 115, No. 2B, 1993, pp. 426–438. https://doi.org/10.1115/1.2899083.

[14] Balas, G. J., "μ-Synthesis," *Control Systems, Robotics, and Automation, Vol. IX*, Encyclopedia of Life Support Systems (EOLSS), 2009, pp. 152–167.

[15] Mathworks, "MATLAB® Robust Control Toolbox," 2021. URL https://www.mathworks.com/products/robust.html.